This is the accepted manuscript made available via CHORUS. The article has been published as:

Ultrathin limit and dead-layer effects in local polarization switching of BiFeO_{3}

Peter Maksymovych, Mark Huijben, Minghu Pan, Stephen Jesse, Nina Balke, Ying-Hao Chu, Hye Jung Chang, Albina Y. Borisevich, Arthur P. Baddorf, Guus Rijnders, Dave H. A. Blank, Ramamoorthy Ramesh, and Sergei V. Kalinin

Phys. Rev. B **85**, 014119 — Published 31 January 2012

DOI: 10.1103/PhysRevB.85.014119

Resubmitted: Physical Review B

Date: 09/23/2011

Revised: 11/22/11

The Ultrathin Limit and Dead-layer Effects in Local Polarization Switching of $BiFeO_3$

Peter Maksymovych[1]*, Mark Huijben[2,3], Minghu Pan[1], Stephen Jesse[1], Nina Balke[1], Y. H. Chu[4], Hye Jung Chung[5], Albina Y. Borisevich[5], Arthur P. Baddorf[1], Guus Rijnders[2], Dave H. A. Blank[2], Ramamoorthy Ramesh[3] and Sergei V. Kalinin[1]

[1] Center for Nanophase Materials Science, Oak Ridge National Laboratory, Oak Ridge, TN, 37831

[2]Faculty of Science and Technology, MESA+ Institute for Nanotechnology, University of Twente, P. O. Box 217, 7500 AE Enschede, the Netherlands

[3]Department of Materials Sciences and Engineering and Department of Physics, University of California Berkeley, Berkeley, CA, 94720

Department of Materials Science and Engineering, National Chiao Tung University, HsinChu, 30010, Taiwan

[5] Materials Science and Technology Division, Oak Ridge National Laboratory, Oak Ridge, TN, 37831

*corresponding author: maksymovychp@ornl.gov

Abstract

Using piezoresponse force microscopy in ultra-high vacuum, polarization switching has been detected and quantified in epitaxial $BiFeO_3$ films from 200 unit cells down to about 4 unit cells thick. Local remnant piezoresponse was utilized to probe both ferroelectric properties as well as the effects of imperfect electrical contacts. It was found that the shape of the electromechanical hysteresis loops is strongly influenced by an extrinsic dielectric gap, primarily through the suppressing effect of the depolarizing field on the spontaneous polarization in the ultrathin films. Furthermore, statistical analysis of hysteresis loops has revealed lateral variation of the extrinsic dielectric gap with sub-10 nm resolution. Robust and reproducible ferroelectric properties of nanoscale $BiFeO_3$ indicate its potential for nanoscale applications in information storage and spintronics.

1. Introduction

Ferroelectric materials and polarization switching in confined geometries have strong potential for information storage [1,2], energy storage [3], opto-electronic and spintronic applications [4,5]. At the same time, ferroelectricity is subject to pronounced size effects, manifested as the scaling of the magnitude of ferroelectric polarization [6,7], and the scaling of the coercive field that triggers polarization switching [8-11], as well as the evolution of the polarization domain morphology with the size [12,13] and dimensionality [14,15] of ferroelectric and multiferroic materials. Although ferroelectric size-effects have been investigated for many decades [16,17], many questions still remain open or controversial.

One such question, which pertains to many prospective ferroelectric applications, is the scaling of the coercive field (E_c) with film thickness (h) or dimensionality. For macroscopic films, with dimensions far exceeding the correlation length, the coercive field follows the Kay-Dunn law, $E_c \sim h^{-2/3}$ [18], established using the Landauer nucleation model for polarization switching [19]. In the original model, the Kay-Dunn law is expected to break down at an ultrathin limit, because the nucleus shape will change from

the half-prolate Landauer-shape [19] to cylindrical, which in turn will cancel the depolarizing energy of the charged apex. In this case, the coercive field scaling is expected to saturate at a certain value. While this scenario was invoked by Jo et. al [8] to explain the saturation of the field in epitaxial $BaTiO_3/SrRuO_3$ capacitors below ~ 10 nm, other authors based on the studies of a ferroelectric polymer PVDF [10], have claimed that the saturation signals the onset of intrinsic ferroelectric switching, where the direction of spontaneous polarization is reversed uniformily throughout the film rather than through the nucleation-growth mechanism. Finally, Dawber et. al [11] suggested that Kay-Dunn scaling in PVDF switching should be recovered down to as low as 1 nm by including the effect of the dielectric dead-layer and the depolarizing field in the polymer film.

Reliable interpretation of size-dependent ferroelectric switching requires the knowledge of the electric field inside the ferroelectric volume. However, the electric field is in general non-uniform throughout the ferroelectric capacitor, due to dead-layers (manifested as dielectric gaps in the contact region among other effects), dopant profiles and space-charge regions, the properties of which are largely unknown. The problem is further complicated because conventional P-E hysteresis measurements based on displacement current are not explicitly sensitive to dielectric gaps [20]. The resulting uncertainty in the interpretation will become most pronounced at the ultrathin limit, where extrinsic effects will dominate the electric field profile.

Here we have studied the properties of ferroelectric switching in ultrathin films using the magnitude and hysteresis of piezoresponse (strain due to applied electric field) [21], rather than those of the displacement current as in conventional P-E measurements. Under a reasonable assumption that the overall piezoresponse will be dominated by the ferroelectric volume, the magnitude of piezoresponse provides a direct measure of the electric field inside the ferroelectric. Systematic analysis of piezoresponse hysteresis loops has allowed us to detect remnant and switchable polarization down to 4 unit cells (1.6 nm) in epitaxial films of $BiFeO_3$, infer the presence of the dielectric gaps and the intrinsic ferroelectric behavior. Furthermore, we have, for the first time, spatially resolved the variation of the dielectric gap effects with < 10 nm resolution.

2. Experimental

$BiFeO_3$ (BFO) films were deposited on 5 nm conducting $La_{0.7}Sr_{0.3}MnO_3$ (LSMO) electrodes by pulsed-laser deposition (PLD) with reflection high-energy electron diffraction (RHEED) control of the growth process, at 750 °C and P_{O2} = 200 mTorr for LSMO and 670 °C and P_{O2} = 100 mTorr for BFO [22, 23]. After the growth, the heterostructures were slowly cooled to room temperature in 1 atm of oxygen at a rate of ~5 K/min. Film thicknesses were determined from RHEED analysis during PLD growth, and independently confirmed by transmission electron microscopy and X-ray ellipsometry on representative samples. BFO films (except 12 nm and 50 nm) were first annealed at ~ 350 °C and $p(O_2)$ = 10 mTorr to remove surface contamination, while preventing film decomposition and changes of stoichiometry (see below), and then introduced into the vacuum microscope chamber without exposure to ambient. The high crystalline quality of the films was supported by X-ray diffraction (Fig 1a), atomic force microscopy exhibiting flat topography with unit-cell high steps (as seen in Fig. 1(b) for a representative 5 nm film) and transmission electron microscopy (Fig. 1c).

Piezoresponse and ferroelectric switching were characterized using piezoresponse force microscopy (PFM) in ultrahigh vacuum (UHV) at the background pressure of $\sim 2\times10^{-10}$ Torr as described elsewhere [24]. Local piezoresponse hysteresis loops were acquired by applying DC-bias-pulses of increasing magnitude to the tip (Pt-coated Mikromasch CSC37) and measuring the out-of-plane *remnant* piezoresponse between the pulses. Although we did not directly control the size and curvature of the AFM tip, which determines the spatial distribution and strength of applied electric field, we estimated it to be much larger (> 25 nm) than the thickness of the ultrathin films (except for the 50 nm film), and we did not detect any significant difference in the switching behavior obtained with different tips.

The measurement sensitivity was maximized using the band-excitation technique [25], where the cantilever is excited by a band of frequencies in the vicinity of the first contact resonance (Fig.2a,b). Fig. 2a shows a typical hysteresis measurement on a 2.8 nm BFO film and the hysteresis loops (Fig. 2c) extracted by integrating the response in the probed frequency range.

3. Results

3.1. Average thickness-dependence of local ferroelectric switching

Although PFM methodology was applied to ultrathin $BiFeO_3$ and $PbTiO_3$ films as well as nanoparticles in previous works [7,22,27,28,29,30], all such measurements were carried out in ambient environment and could thus be compromised by extrinsic local electrochemical reactions, particularly in the thickness range <10 nm as previously noted for BFO [22] and other perovskite surfaces [31]. Furthermore, only *in-field* piezoresponse [22,30] was used to infer ferroelectric switching in ultrathin films, leaving uncertain the existence of switchable remnant polarization and the respective size-effects.

Here, the piezoresponse hysteresis loops corresponding to the switching of remnant out-of-plane polarization were reproducibly observed down to the thinnest, 1.6 nm film BFO film (Fig. 3a). The hysteresis loops on two separate 2 nm films, only one of which had been annealed in vacuum, were nearly identical (Fig. 3b), indicating that the measured properties were intrinsic to as-grown films. Finally, very good reproducibility of the hysteresis loops in consecutive switching cycles (Fig. 2a,c) and negligible variation of the contact resonance frequency during ferroelectric switching (Fig. 2d) testified to the lack of surface damage and electrochemical reactions during ferroelectric switching. At the same time, we have verified that spontaneous polarization of the 2 nm (Fig. 3c,d) and 5 nm (not shown) BFO films could be reversed in a large surface area (~ 90×140 nm^2 for the 2 nm film) by poling it with a biased tip. Altogether, we conclude that epitaxial BFO retains ferroelectricity down to at least 1.6 nm.

Comparative statistics for the thickness-dependence of ferroelectric switching was derived from 30-100 hysteresis loops from each film. Each hysteresis loop was fitted with a phenomenological function (Fig. 2c) to extract the switching bias [25]. The average hysteresis loops, Fig. 3a, revealed rapid drop-off of remnant piezoresponse with decreasing film thickness (Fig. 3b), as well as significant lowering of the switching bias. Given the imperfections in the chemical stoichiometry found at the interfaces of epitaxial oxide films, as well as the non-epitaxial top contact (tip-surface), it is reasonable to assume the existence of the dielectric gaps within the Pt-tip-BFO-LSMO nanocapacitor, that will lower the electric field inside the BFO film compared to the perfect-contact scenario [11] and could explain the observed trend. In this case, the normal component of

the electric field inside the film (E_z) can be approximated by a capacitor model with dielectric gaps [20]

$$E_z = \frac{U\varepsilon_d}{\varepsilon_d h + \varepsilon_h^b d} - \frac{P_z d}{\varepsilon_0\left(\varepsilon_d h + \varepsilon_h^b d\right)} \qquad \text{eq. (1)}$$

where d – total thickness of the dielectric gaps, U – potential across the film, P_z – out-of-plane polarization component, ε_d - dielectric constant of the dead layer (assumed the same for top and bottom layers), ε_h^b - dielectric background constant of the ferroelectric/piezoelectric volume, that is independent on the film thickness in contrast to dielectric permittivity ε_{33}^f part related with the soft mode.

The thickness of the dielectric gaps (d) is not known a-priori, presenting a major problem for the quantitative interpretation of the ferroelectric hysteresis loops from ultrathin films (particularly the thickness dependence of the switching voltage), obtained both locally as in our experiments and in capacitor measurements with fixed electrodes. However, local piezoresponse is a second independent observable which can potentially provide the much needed information on the scaling of the electric field profile and/or polarization across the thickness range or, in fact, across the surface of the ferroelectric film.

Assuming uniform polarization perpendicular to the film's surface, the out-of-plane piezoelectric strain produced in the tetragonal film by applied electric field can be expressed as $u_z \propto h \cdot E_z \varepsilon_{33} \varepsilon_0 Q_{11} P_z$, where E_z is the electric field inside the ferroelectric, ε_{33} and Q_{11} are the components of the dielectric and electrostrictive tensors, respectively. Experimentally, the out-of-plane piezoresponse is measured approximately as a first derivative of the out-of-plane piezoelectric strain with respect to applied bias, $\partial u_z / \partial V$. Thus, if we were to assume a linear potential drop across the whole Pt-tip/BFO/LSMO structure (a perfect contact scenario) with a corresponding out-of-plane electric field component of $E_z = U/h$, the measured piezoresponse would depend *only* on the magnitude of spontaneous polarization, P_z. The dielectric gaps located at the interfaces will: (a) lower the electric field inside the ferroelectric volume (eq.1) and (b) suppress the mangnitude of spontaneous polarization due to the depolarizing field (the second term in eq.1). Therefore in the presence of the dielectric gaps, both pure electrostatics of the

junction and the scaling of the ferroelectric properties of the film will contribute to the overall thickness-dependence of piezoresponse (in a more general case, intrinsic scaling of the dielectric properties and the polarization itself will also contribute to the thickness dependence of piezoresponse). To analyze this problem further, we first introduce the relevant aspects of the intrinsic model for ferroelectric switching [26] in the context of finite film thickness and interfacial dielectric gaps. Our previous experiments [24,32] have shown that intrinsic switching is the dominant mechanism for polarization reversal in PFM measurements.

5. Model for thickness-dependence of intrinsic switching

The 1D model detailed here is applicable until $h << R$, i.e. for film thickness (h) smaller than the tip raidus (R). Since R > 25 nm (see Appendix A) the model can be applied to all studied BFO films, with a possible exception of the 50 nm film. The presence of the thickness dependent depolarization field self-consistently reduces the polarization value P_z via the ferroelectric equation of state with cubic nonlinearity [26]:

$$\alpha\langle P_z\rangle + \beta\langle P_z^3\rangle = \langle E_z\rangle + E_b \tag{2}$$

Here we use the average polarization $\langle P_3\rangle \equiv \frac{1}{h}\int_0^h P_3(\tilde{z})d\tilde{z}$. The built-in field E_b is proportional to the built-in potential and polarization contributions: $E_b = \frac{\varepsilon_d U_b}{\varepsilon_d h + \varepsilon_h^b d} - \frac{P_b}{\varepsilon_0 \varepsilon_h^b}$. Then, Eq.(2) can be rewritten including renormalized coefficient $\alpha_R = \alpha + \frac{1}{\varepsilon_0}\frac{d}{\varepsilon_d h + \varepsilon_h^b d}$ as

$$\alpha_R\langle P_z\rangle + \beta\langle P_z^3\rangle = \frac{U\varepsilon_d}{\varepsilon_d h + \varepsilon_h^b d} + E_b \tag{3}$$

Then thermodynamic or intrinsic coercive bias becomes

$$\begin{aligned} E_c^b &= -E_b \pm \frac{2}{3\sqrt{3}}\sqrt{-\frac{\alpha_R^3}{\beta}} = -E_b \pm E_c^0\left(1 + \frac{1}{\alpha\varepsilon_0}\frac{d}{\varepsilon_d h + \varepsilon_h^b d}\right)^{3/2} \\ &\underset{\varepsilon_d h >> \varepsilon_h^b d}{\approx} -E_b \pm E_c^0\left(1 + \frac{1}{\alpha\varepsilon_0}\frac{d}{\varepsilon_d h}\right)^{3/2} \sim E_c^0\left(1 - \frac{h_{cr}^{eff}}{h}\right)^{3/2} \end{aligned} \tag{4}$$

where the bulk thermodynamic coercive field is $E_c^0 = \frac{2}{3\sqrt{3}}\sqrt{-\frac{\alpha^3}{\beta}}$ (for BFO it is about 5×10^8 V/m) and $h_{cr}^{eff} = \frac{-d}{\alpha\varepsilon_0\varepsilon_d}$ is the critical thickness for ferroelectricity. Using Eq.(4) one can estimate the intrinsic thermodynamic switching bias as

$$U_c = E_c^b h \sim h\left(1-\frac{h_{cr}^{eff}}{h}\right)^{3/2} \qquad (5)$$

At the same time, the values for spontaneous polarization are given by

$$P_z\left(E_b = 0, U = 0\right) = \pm\sqrt{-\frac{\alpha_R}{\beta}} = \pm P_S^b\sqrt{1+\frac{1}{\alpha\varepsilon_0}\frac{d}{\varepsilon_d h+\varepsilon_h^b d}} \underset{\varepsilon_d h>>\varepsilon_h^b d}{\approx} \pm P_S^b\sqrt{1-\frac{h_{cr}^{eff}}{h}} \qquad (6)$$

where the bulk spontaneous polarization is $P_S^b = \sqrt{-\frac{\alpha}{\beta}}$.

Within the LGD approach, the out-of-plane strain u_{zz} and piezoresponse u_z of a tetragonal film are

$$u_{zz} = \varepsilon_{33}^f\varepsilon_0 Q_{11}P_z E_z,$$

$$u_z \approx \int_0^h \varepsilon_{33}^f\varepsilon_0 Q_{11}P_z E_z dz \sim \varepsilon_0 Q_{11}\frac{\varepsilon_{33}^0 h}{1-h_{cr}^{eff}/h}\frac{U\varepsilon_d}{\varepsilon_d h+\varepsilon_h d}P_S^b\sqrt{1-\frac{h_{cr}^{eff}}{h}} \sim \frac{U}{\sqrt{1-h_{cr}^{eff}/h}} \qquad (7)$$

Under the assumption of constant dielectric permittivity ε_{33}^f, the piezoresponse is given by

$$u_z = U\sqrt{1-\frac{h_{cr}^{eff}}{h}} \qquad (8)$$

Equation 8 can fit the experimentally observed thickness dependence of piezoresponse reasonably well, as seen in Fig. 4a. The corresponding critical thickness, h_{cr}^{eff}, lies in the range from 1 to 2 nm, which by itself is, of course, consistent with our observation of ferroelectric switching in $BiFeO_3$ down to at least 1.6 nm. Using the bulk value for α ($\alpha = -8\cdot10^8$ m/F) and assuming ε_d between 1 and 4, the corresponding

thickness of the dead-layers is between 0.01 and 0.03 nm. Therefore, the dielectric gaps are very thin in this case and the scaling mainly arises from the effect of the depolarizing field on the spontaneous polarization, rather than the electrostatic attenuation of the applied electric field inside the ferroelectric volume.

Equation 5 predicts that the nucleation bias scales linearly with the film thickness, deviating from linearity only when the thickness approaches the critical value h_{cr}^{eff}. The slope equals the coercive field in the bulk, or the region of the film far away from the interfaces. As seen in Fig. 4c, the experimental thickness dependencies of both positive and negative switching bias are indeed linear in almost all the measured range. The slopes are ~ 47 MV/m for the negative and ~ 58 MV/m for the positive switching bias, respectively. Assuming intrinsic switching and the bulk dielectric constant of $30\varepsilon_0$ [33], these values correspond to a spontaneous polarization of ~ 25 μC/cm^2 along the <111> direction. This value is 3-5 fold smaller than the reported values for the $BiFeO_3$ bulk [33], but we consider the agreement to be satisfactory given the simplifying assumptions of our procedure, and the fact that polarization can be smaller in our particular thin films that the record values obtained for bulk or thick films of BFO.

A more significant disparity between theory and experiment is observed in the intercept of the magnitude of switching bias at zero thickness. According to Eq. 5, the maximum intercept is zero (at zero h_{cr}^{eff}). At non-zero critical thickness, switching bias becomes complex below h_{cr}^{eff}, formally translating into a negative intercept. The inspection of Fig. 4c reveals that (ignoring the two thinnest films) the scaling of the positive nucleation bias intercepts the y-axis at approximately zero, which is consistent with the very thin dielectric gaps estimated from the thickness-dependence of piezoresponse. However, the values for the magnitude of the negative nucleation bias have a positive intercept.

Although at present we cannot explain the origin of the large intercept, we would like to note that it has a dramatic effect on the scaling of the apparent switching field, which is usually calculated as U_c/h (valid only in the limit of zero dielectric gap as we discussed before). Calculating the apparent switching field from our data (Fig. 4d) reveals that the positive switching field remains approximately constant across the thickness

range, as expected based on the intrinsic switching model. However, due to a non-zero intercept the negative switching field scales approximately as $E_c \propto h^{-0.75\pm0.04}$, which is very a similar trend to the well-known Kay-Dunn law (coercive field $\propto h^{-0.66}$) derived for macroscopic films [18]. The Kay-Dunn law should not apply for ultrathin films where the polarization nucleus becomes cylindrical [8]. Furthermore, within the intrinsic model, the growth of the switching field with decreasing thickness implies an *increase* of spontaneous polarization, because as discussed above $|P_z| = \sqrt{-\frac{\alpha}{\beta}}$ and the coercive field $E_c^0 = \frac{2}{3\sqrt{3}}\sqrt{-\frac{\alpha^3}{\beta}}$ (α and β are the first and second coefficients in the Landau-Giznburg-Devonshire equation of state). This would starkly contradict simultaneous piezoresponse measurements (Fig. 3a), which imply that polarization *decreases* with decreasing thickness. Piezoreponse measurements therefore provide sufficient self-consistency to rule out the rapid increase of the apparent switching field with decreasing film thickness.

6. Spatially resolved analysis of ferroelectric switching

Given the sensitivity of remnant piezoresponse to the properties of the dielectric gaps discussed in the previous sections, we anticipated that there would be some observable variation among local hysteresis loops across the surface. To verify this hypothesis, we acquired 9600 hysteresis loops on a grid of 80x40 points with a spatial resolution of 2 nm per pixel on the surface of the 2 nm $BiFeO_3$ film. As seen in Fig. 5a systematic variations were indeed observable, with about two-fold variation of piezoresponse magnitude across the surface, but well within the measurement accuracy. Notably the changes were not all random, with piezoresponse on average smaller at the bottom and top of the map (green) and larger (red) in the middle, Fig. 5a. The pronounced regions of zero piezoresponse (blue) in Fig. 5a correspond to defects on the surface where no hysteresis loop opening was observed. They are not discussed here further.

The streakiness of some of the lines in Fig. 5(a) indicates abrupt changes between consecutive lines across the surface, which suggests that the changes in the critical thickness, and the corresponding dielectric gaps are occurring at the top (Pt-BFO), rather than bottom (BFO-LSMO) interface. If we were to attribute the observed variations to subtle changes in the dielectric gap, the ratio of piezoresponse values from two different locations on the surface would be $\frac{u_{z1}}{u_{z2}} = \sqrt{\frac{h - h_{cr1}^{eff}}{h - h_{cr2}^{eff}}}$. Although we don't have an independent measure of the respective critical thicknesses, for a 2 nm film, a two-fold suppression of piezoresponse would be produced by increasing the critical thickness by a factor of 1.2 to 1.8 for the range of critical thicknesses from 1.6 to 1 nm (a range derived earlier and consistent with the film thickness range studied here).

Thus piezoresponse mapping appears to be a very sensitive probe of the local junction properties, particularly at the ultrathin limit. With increasing film thickness, the sensitifivity of piezoresponse to the changes of the critical thickness diminishes. Prospectively, this trend can be used to differentiate local changes of the dielectric gap from surface-specific variations (e.g. contact potential difference, electrochemistry etc.), which will present on the surface irrespective of film thickness. We would like to emphasize that the extrinsic dead layer (which is very likely going to be present in most measurements, particularly in ambient or liquids) does not impede ferroelectricity down to a length-scale of the unit-cell. Furthermore we observe that the absolute width of the distribution of the switching bias for ultrathin films is about ±0.1 V (Fig. 5b), which is about an order of magnitude smaller than that for 50 nm $BiFeO_3$ films (±1 V [24]). This fact has important practical implications for the reproducibility of devices based on nanoscale ferroelectrics.

7. Conclusions

In summary, we have presented the first systematic and statistical analysis of the remnant piezoresponse hysteresis loops measured on a series of epitaxial thin films of BFO from 50 nm down to 1.6 nm. All the $BiFeO_3$ films were found to be repeatedly and

reproducibly switchable, demonstrating the feasibility of nanoscale ferroelectricity for the fundamental studies and device applications replying on polarization switching, such as polarization-controlled electron transport and ultrahigh density information storage [1]. Using the magnitude of piezoresponse to probe ferroelectricity as well as the electrostatic properties of the ferroelectric junction, we have inferred that the shape of the ferroelectric hysteresis loop is primarily influenced by the extrinsic dielectric gaps at the films' interfaces, which, in turn, suppress spontaneous polarization through the effect of the depolarizing field. An overall good agreement was obtained between experimentally observed scaling of piezoresponse and switching field and the intrinsic model for ferroelectric switching. Thus we have been also able to estimate the magnitude of spontaneous polarization in the studied films. However, the model cannot at present explain the offset in the switching bias for one of the switching polarities. Most notably, this offset gives rise to a spurious Kay-Dunn-like scaling of the switching field. At the same time, the scaling can self-consistently ruled out by the corresponding scaling of piezoresponse. Finally, we have demonstrated spatially-resolved mapping of the extrinsic dielectric gap within nanometer-scale resolution based on the variations of individual ferroelectric hysteresis loops across the surface. The observed variations are consistent with our assignment of the imperfect tip-surface contact as the origin of the extrinsic dielectric gap. Such systematic measurements of nanoscale ferroelectricity now pose a possibility of exploring the scaling of the multiferroic properties of $BiFeO_3$ down to a few unit cell thickness. On the other hand, careful tip- and surface preparation can prospectively eliminate the extrinsic dielectric gap, and allow a more rigorous comparison between experiment and theory, including a possibility of increased piezoresponse with decreasing film thickness motivated by the intrinsic model.

Acknowledgements

PFM experiments were carried out at the Center for Nanophase Materials Sciences, Division of User Facilities, U.S. Department of Energy. The work at Berkeley is supported by the Director, Office of Science, Office of Basic Energy Sciences, Materials Sciences Division of the U.S. Department of Energy under contract No. DE-AC02-05CH1123.

Appendix A

To support our use of the 1D approximation for the electrostatics of the problem, we estimated the tip size based on the width of the domain wall profile as detailed in [34] Figure 5 shows the image of the poled domain structure on a reference 50 nm epitaxial film of $PbZr_{0.2}Ti_{0.8}O_3$ and line-profiles of the corresponding domain walls. The domain wall profile was fitted using the following equation [34]:

$$u(x) \approx u_0 + \alpha\left[\frac{3}{4}\left(d_{33} + \left(\frac{1}{3} + \frac{4}{3}\nu\right)d_{31}\right)\frac{(x-x_0)/r}{|(x-x_0)/r| + 1/4} + \frac{1}{4}d_{15}\frac{(x-x_0)/r}{|(x-x_0)/r| + 3/4}\right]$$

where *u(x)* is the measured piezoresponse, d_{ij}– piezoelectric coefficients, ν - Poisson ratio. α – proportionality coefficient, x_0 – relative center of the domain wall, and $r = 2R_d/\pi$, where R_d is the disk radius assuming a model of a disk and a single image charge description of the localized electric field, are all fitting parameters [34]. Based on the reasonably good fit (Fig. 6), the radius of the disk (approximating the AFM tip apex) equals 25 nm and 29 nm for the two walls, which is also in good agreement with the width of the domain walls (~29 nm and ~33 nm, respectively). Therefore, our typical effective tip size is much larger than the thickness of all the ultrathin films (with the exception of the 50 nm $BiFeO_3$ film, which is used only as a reference). Thus, the relatively large tip size justifies the use of the 1D approximation for the electric field in this study. Parenthetically, the effective tip size in ultrahigh vacuum is approximately two-fold smaller than in the ambient environment.

References

[1] E. Y. Tsymbal, H. Kohlstedt. *Science* **313**, 181 (2006).

[2] I. I. Naumov, L. Bellaiche, H. X. Fu, *Nature* **432**, 737 (2004).

[3] L. Yu, V. Ranjan, M. B. Nardelli, J. Bernholc, *Phys. Rev. B*. **80**, 165432 (2009).

[4] M. Gajek, M. Bibes, S. Fusil, K. Bouzehouane, J. Fontcuberta, A. Barthélémy, A. Fert, *Nat. Mat.* **6**, 296 (2007).

[5] J. P. Velev, C. Velev, J. D. Burton, A. Smogunov, M. K. Niranjan, E. Tosatti, S. S. Jaswal, E. Y. Tsymbal, *Nano Lett.* **9,** 427 (2009).

[6] J. Junquera, P. Ghosez, *Nature* **422**, 506 (2003).

[7] V. Nagarajan, S. Prasertchoung, T. Zhao, H. Zheng, J. Ouyang, R. Ramesh, W. Tian, X. Q. Pan, D. M. Kim, C. B. Eom, H. Kohlstedt, R. Waser, *Appl. Phys. Lett*. **84**, 5225 (2004).

[8] J. Y. Jo, Y. S. Kim, T. W. Noh, J. Yoon, T. K. Song, *Appl. Phys. Lett*. **89**, 232909 (2006).

[9] A. N. Morozovska, E. A. Eliseev, Y. Li, S. V. Svechnikov, P. Maksymovych, V. Y. Shur, V. Gopalan, L. Chen, S. V. Kalinin, *Phys. Rev. B* **80***,* 214110 (2009).

[10] S. Ducharme, V. Fridkin, A. Bune, S. Palto, L. Blinov, N. Petukhova, S. Yudin, *Phys. Rev. Lett.* **84**, 175 (2000).

[11] M. Dawber, P. Chandra, P. Littlewood, J. Scott, *J. Phys. Cond. Mat.* **15**, L393 (2003).

[12] G. Catalan, H. Béa, S. Fusil, M. Bibes, P. Paruch, A. Barthélémy, J. Scott, *Phys. Rev. Lett*. **100**, 027602 (2008).

[13] D. D. Fong, G. Stephenson, S. Streiffer, J. A. Eastman, O. Auciello, P. H. Fuoss, C. Thompson, *Science* **304**, 1650 (2004).

[14] S. H. Baek, H. W. Jang, C. M. Folkman, Y. L. Li, B. Winchester, J. X. Zhang, Q. He, Y. H. Chu, C. T. Nelson, M. S. Rzchowski, X. Q. Pan, R. Ramesh, L. Q. Chen, C. B. Eom, *Nat. Mat*. **9**, 309 (2010).

[15] J. E. Spanier, A. M. Kolpak, J. J. Urban, I. Grinberg, L. Ouyang, W. S. Yun, A. M. Rappe, H. Park, *Nano Lett*. **6**, 735 (2006).

[16] M. Dawber, K. M. Rabe, J. Scott, *Rev. Mod. Phys.* **77**, 1083 (2005).

[17] T. Shaw, S. Trolier-McKinstry, P. McIntyre, Ann. Rev. Mat. Sci. **30**, 263 (2000).

[18] H. F. Kay, J. W. Dunn, *Phil. Mag.* **7,** 2027 (1962).

[19] Landauer, R. *J. Appl. Phys.* ***28***, 227 (1957).

[20] A. M. Bratkovsky, A. P. Levanyuk, *J. Comp. Theor. Nanosci*. **6**, 465 (2009).

[21] S. V Kalinin, B. J. Rodriguez, S. Jesse, P. Maksymovych, K. Seal, M. Nikiforov, A. P. Baddorf, A. L. Kholkin, R. Proksch, *Mat. Today* **11**, 16 (2008).

[22] Y. H. Chu, T. Zhao, M. P. Cruz, Q. Zhan, P. L. Yang, L. W. Martin, C. H. Yang, F. Zavaliche, H. Zheng, R. Ramesh, *Appl. Phys. Lett*. **90**, 252906 (2007).

[23] M. Huijben, L. W. Martin, Y.-H. Chu, M. B. Holcomb, P. Yu, G Rijnders, D. H. Blank, R. Ramesh, *Phys. Rev. B*. **78**, 094413 (2008).

[24] P. Maksymovych, S. Jesse, M. Huijben, R. Ramesh, A. Morozovska, S. Choudhury, L. Chen, A. P. Baddorf, S. V. Kalinin, *Phys. Rev. Lett.* **102**, 017601 (2009).

[25] S. Jesse, P. Maksymovych, S. V. Kalinin, *Applied Physics Letters*. **93**, 112903 (2008).

[26] A. N. Morozovska, E. A. Eliseev, Y. Li, S. V. Svechnikov, A. D. Krutov, V. Y. Shur, A. Y. Borisevich, P. Borisevich, S. V. Kalinin, *Phys. Rev. B* **81**, 205308 (2009).

[27] D. D. Fong, A. M. Kolpak, J. A. Eastman, S. K. Streiffer, P. H. Fuoss, G. B. Stephenson, C. Thompson, D. M. Kim, K. J. Choi, C. B. Eom, I. Grinberg, A. M. Rappe, *Phys. Rev. Lett.* **96**, 127601, 2006.

[28] H. Béa, S. Fusil, K. Bouzehouane, M. Bibes, M. Sirena, G. Herranz, E. Jacquet, J. Contour, A. Barthélémy. *Jap. J. Appl. Phys*. **45**, L187 (2006).

[29] T. Tybell, C. Ahn, J. Triscone, *Appl. Phys. Lett.* **75**, 856 (1999).

[30] H. Fujisawa, M. Okaniwa, H. Nonomura, M. Shimizu, H. Nlu, *J. Eur. Ceram. Soc*. **24** (2004) 1641-1645.

[31] Y. Xie, C. Bell, T. Yajima, Y. Hikita, H. Y. Hwang, *Nano Lette*. **10** (2010) 2588.

[32] S. V. Kalinin, B. J. Rodriguez, S. Jesse, Y. H. Chu, T. Zhao, R. Ramesh, S. Choudhury, L. Chen, E. A. Eliseev, A. N. Morozovska, *PNAS* 104, 20204 (2007).

[33] G. Catalan, J. F. Scott, *Adv. Mat*. 21, 2463 (2009).

[34] S. V. Kalinin, S. Jesse, B. J. Rodriguez, E. A. Eliseev, V. Gopalan, A. N. Morozovska, Appl. Phys. Lett. 90, 212905 (2007).

Figure captions

Figure 1. (a) X-ray diffraction analysis of $BiFeO_3(100)/La_{0.7}Sr_{0.3}MnO_3$ films, some of which were subsequently used in PFM measurements. The thickness of $La_{0.7}Sr_{0.3}MnO_3$ is 5 nm for all the $BiFeO_3$ films. Scans are shifted for clearness. (b) AFM topography of the

5 nm $BiFeO_3$ film and its cross section (inset) along the white dashed. (c) Cross-sectional transmission electron microscopy image of the 3.6 nm $BiFeO_3$ film.

Figure 2. (a) Band-excitation piezoresponse force spectroscopy of two consecutive cycles of the tip-bias-induced ferroelectric switching on the surface of a 2.8 nm $BiFeO_3$ film in ultrahigh vacuum. Pseudocolor plots show the frequency spectrum of the amplitude and phase of cantilever oscillation at its first contact resonance frequency (~232 kHz) along the bias-trajectory (b) of ferroelectric switching. (b)The envelope of tip-bias used to locally switch ferroelectric polarization. (c) Average hysteresis loop extracted from (a,b) as at each spectroscopic step. Red-line is a fit using a phenomenological function. (d) Resonance frequency and resonant amplitude of cantielever oscillation along the ferroelectric hysteresis loop.

Figure 3. Average hysteresis loops acquired from 10-30 random locations of the surfaces of $BiFeO_3$ films ranging from 1.6 nm to 12 nm. The loops were acquired using the same physical cantilever in ultrahigh vacuum. (b) Comparison of vacuum piezoresponse hysteresis loops from two 2 nm BFO/LSMO films, only one of which was annealed in vacuum. (c) Piezoresponse amplitude and (d) phase of an upward-polarized ferroelectric domain recorded on the 2 nm film by poling the area in the center at – 0.8 V.

Figure 4. Thickness dependence of piezoresponse (red) predicted by the intrinsic model, eq. 8, with the assumption of a thickness independent background dielectric constant ε_{33}^{f} and h_{cr}^{eff} = 1.88 nm. Blue dots are experimentally measured piezoresponse values from Fig. 3a. Both theoretical and experimental values have been normalized to the piezoresponse at 50 nm. (b) Positive (blue) and negative (red) switching bias as a function of film thickness determined from the hysteresis loops. (c) Linear fitting of the average nucleation bias values for films in the thickness range between 2.8 and 12 nm. (d) Scaling of the apparent switching electric field (calculated as U_c/h) with film thickness for the positive (blue) and negative (red) polarity.

Figure 5. Spatially resolved hysteresis mapping of a 2 nm $BiFeO_3$ film in ultrahigh vacuum. The remnant piezoresponse, (a), extracted from an average of three hysteresis loops at each of the 3200 points of the map. The hysteresis loops did not open in the dark-blue regions due to topographic defects. (b) Distributions of positive and negative switching bias across the surface of the 2 nm film.

Figure 6. Estimating the effective tip size (tip modeled as a disk with radius (R_d) using the width of a ferroelectric domain wall recorded on the surface of a 50 nm PbZrTiO3 epitaxial film in ultrahigh vacuum (images represent the recorded square domain in the amplitude (top) and phase (bottom) of piezoresponse). The plot shows two domain wall profiles extracted approximately along the white dashed lines, and the corresponding fits following the procedure in Appendix A.

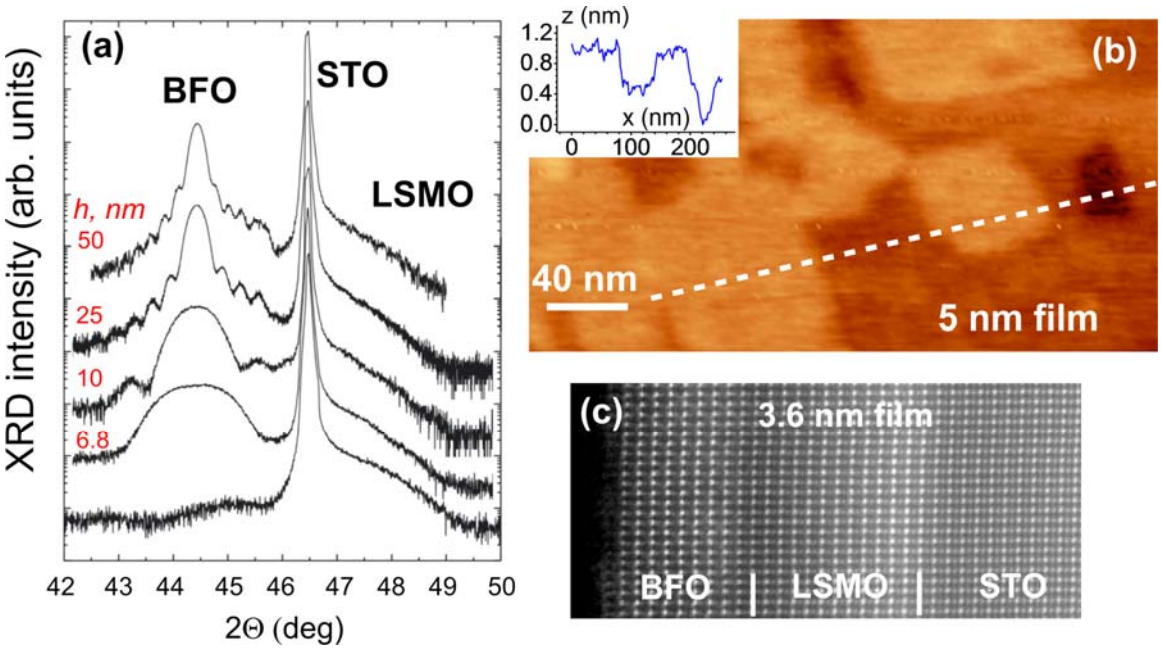

Figure 1. Maksymovych et al.

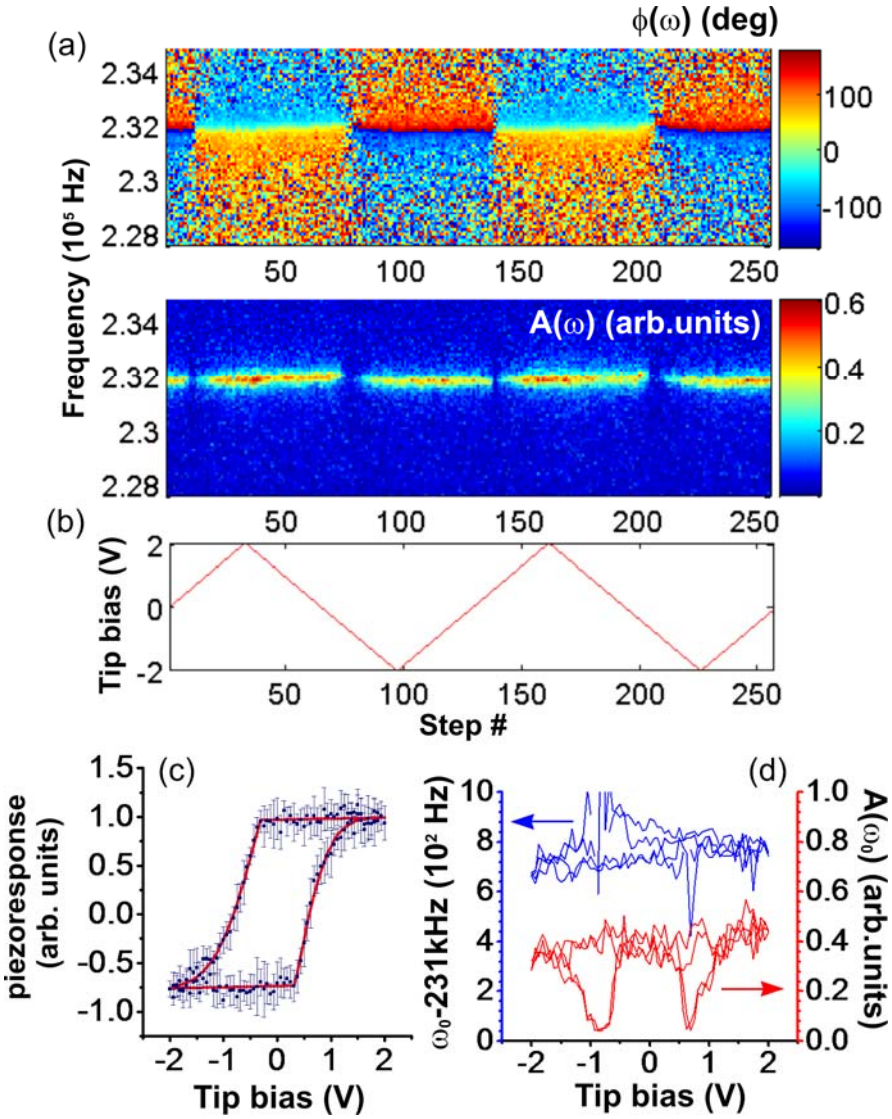

Figure 2. Maksymovych et al.

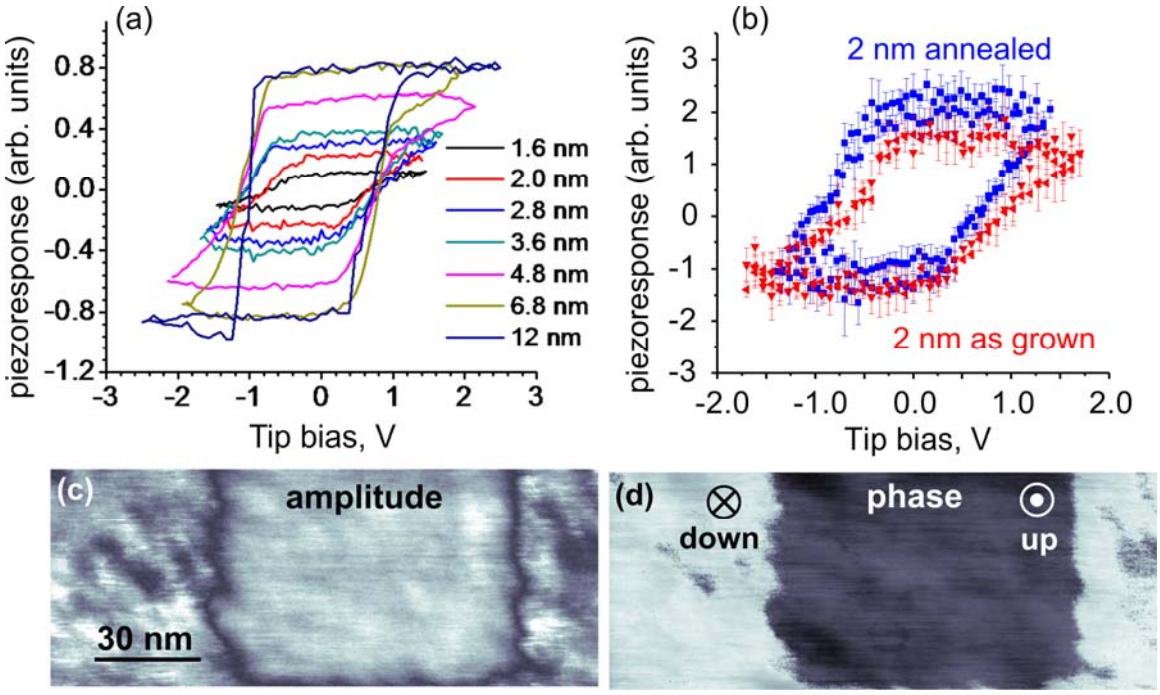

Figure 3. Maksymovych et al.

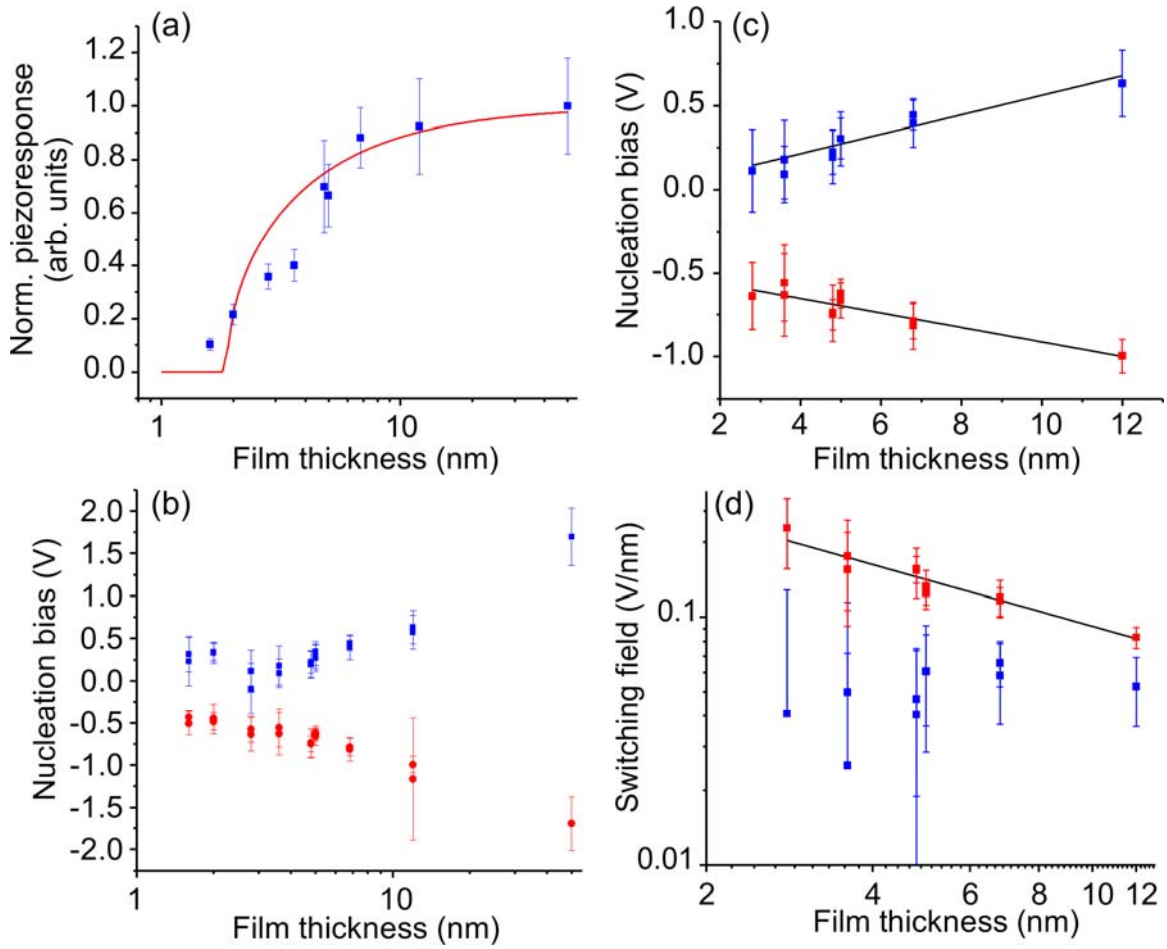

Figure 4. Maksymovych et al.

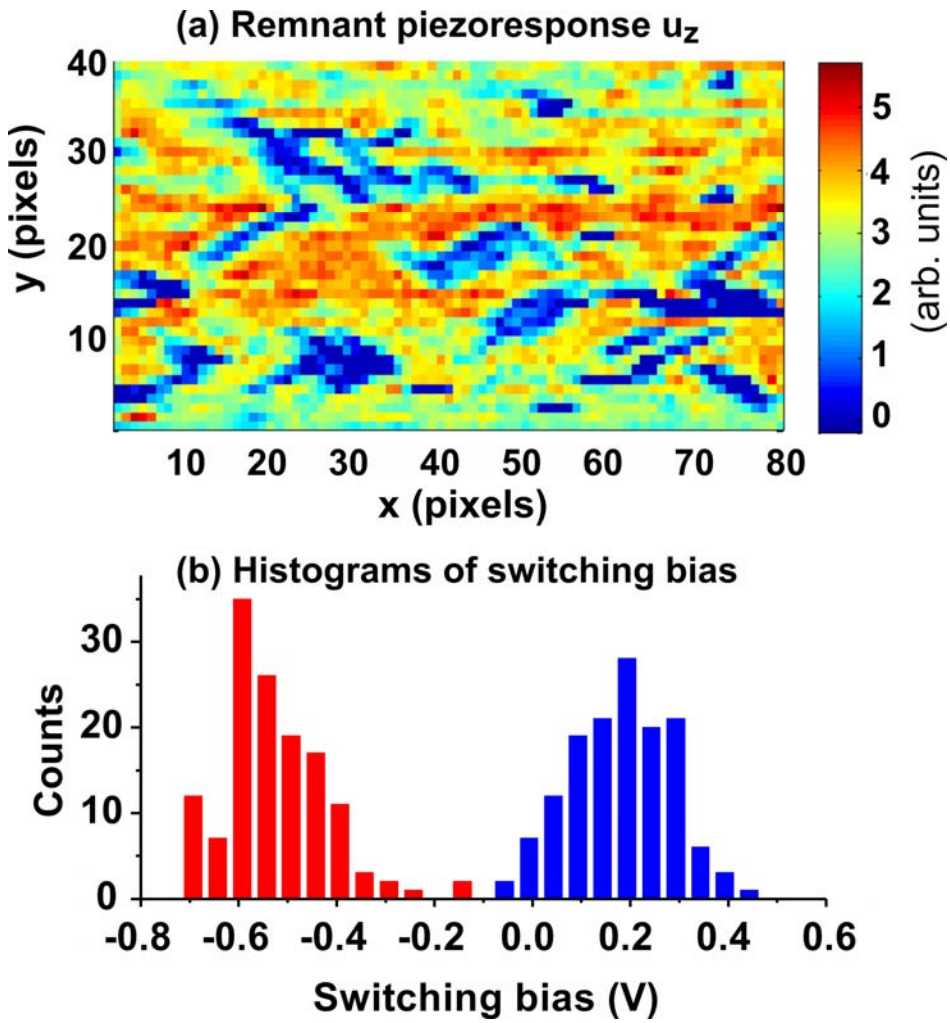

Figure 5. Maksymovych et al.

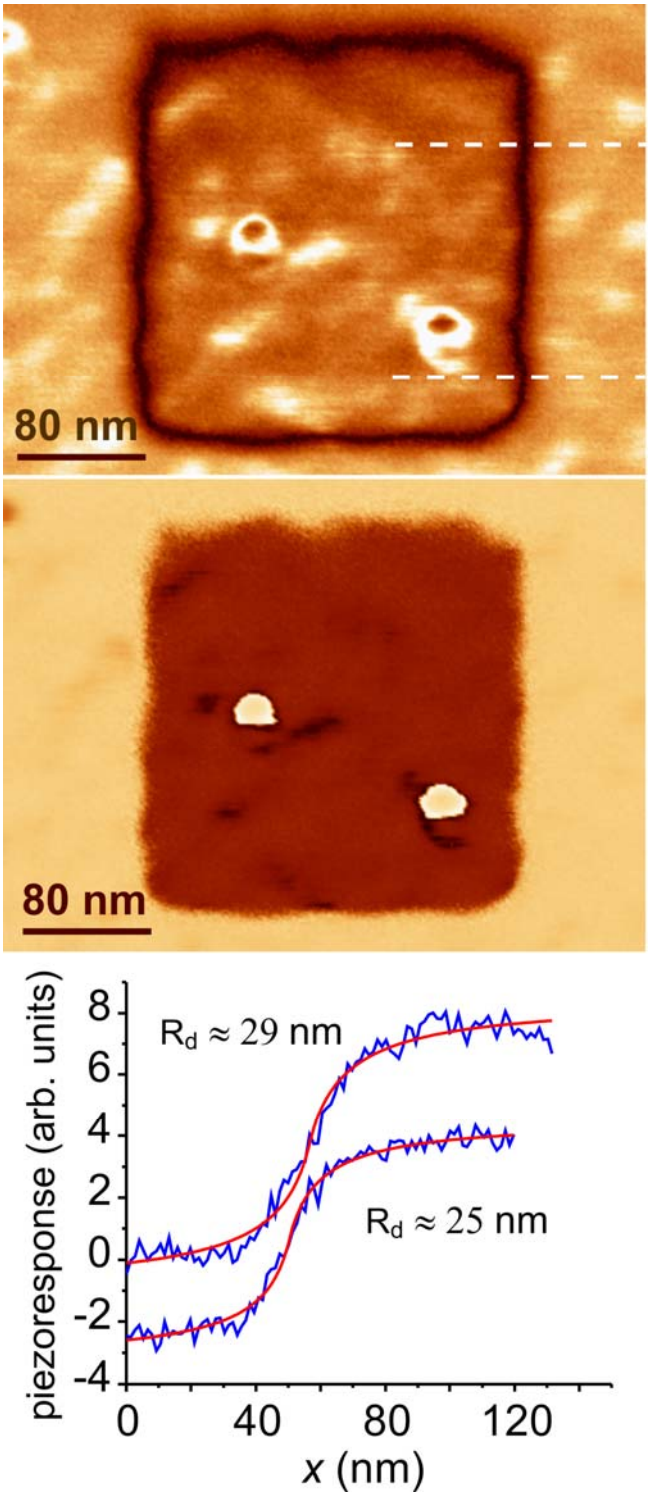

Figure 6. Maksymovych et al.